



Iodine-Induced Gold-Nanoparticle Fusion/Fragmentation/Aggregation and Iodine-Linked Nanostructured Assemblies on a Glass Substrate**

Wenlong Cheng, Shaojun Dong,* and Erkang Wang*

Recently, molecularly bridged nanoparticle aggregates^[1] have been attracting growing interest as a result of their collective electronic, optical, and magnetic properties being distinctly different from a corresponding collection of individual nanoparticles (NPs) or the extended solid. The 2D/3D control over the spatial arrangement of NPs is primarily based on the thiol-amphiphilic nature^[1b,e] of metal NPs, hydrogen-bonding interactions,^[1a] the highly specific recognition interaction of antigens/antibodies, and specific base-pairing interactions^[1f] between DNA and its complementary strand.^[1c,d] In addition, by careful linker-molecule design, spatially and symmetrically well-defined NP aggregates have been reported.^[2] Such aggregated nanostructures can also be constructed on a solid support.^[3] A remaining question is whether atoms can also “glue” NPs together?

A monolayer of iodine atoms has been known to form spontaneously on immersing a bulk-gold surface in dilute iodide solution.^[4] Herein, we demonstrate that such chemisorption also takes place on tiny citrate-stabilized gold NPs. As a result of electron donation, these gold NPs undergo fusion and fragmentation in solution. Also, iodine adsorption on NPs displaces citrate ions from the surface of the NPs and lowers the surface potential, as a result, increasing van der Waals attractive forces between these I-coated gold NPs drive the formation of aggregates in a controlled manner both in solution and on solid support.

The idea that iodide spontaneously chemisorbed on gold NPs was supported by electrochemistry and optical spectra. Using the strategy of Natan and co-workers,^[5] we can prepare highly reproducible NPs submonolayers on 3-aminopropyltrimethoxysilane (APTMS) modified ITO (indium–tin oxide) substrate. The gold NPs submonolayers are rather robust, resistant of electrochemical scanning in the potential range 0–1.5 V (Figure 1a, curve 1). Interestingly, after the NPs submonolayers are immersed into aqueous 1 mM KI solution for several minutes, the submonolayers exhibited characteristic voltammetry of desorption and oxidation of iodine to

iodate (a five-electron process; Figure 1a, curve 2), which is extremely similar to the results obtained with bulk gold.^[4] Thus, it is thought that these APTMS-tethered gold NPs behave in the same way as bulk gold, and a similar chemisorptive process of iodide should take place. The coulometric analysis indicated that a monolayer of adsorbed iodine formed on the exposed surface of the immobilized gold NPs, which is again consistent with the case for bulk gold. This result is also supported by spectral studies. Immersion of gold NP submonolayers in dilute KI leads to gold-surface plasmon-band damping and a red-shift of the peak position (Figure 1b: curve 1)^[6] relative to the original gold plasmon band (Figure 1b: dotted line), which indicates iodine adsorption on these immobilized NPs (see below). Similar spectral responses were also observed for interactions between iodide and free solution-state gold NPs (Figure 1c), which is indicative of similar iodine chemisorptive events on these not-immobilized gold NPs. For confirmation of this result, a control experiment for KCl addition to colloidal Au was performed (Figure 1d); it is clear that no second absorbance band appearance even after 100 μ L of 0.2 M KCl was added. Previous studies^[7] have shown that the interaction of chloride with gold nanoparticles is the result of salt effects. The distinctly different optical responses for KI addition show that iodine interaction must follow a different mechanism. The only reasonable explanation is that a chemisorptive process takes place.

It is expected that the adsorbed iodine on the gold NPs would displace the stabilizing citrate ions, neutralize surface charge, lower “ ζ potential”, thus, paving way for gold-NP aggregation and fusion. This speculation was supported by the optical spectra and transmission electron microscopy (TEM). When controlled amounts of 0.2 M KI were added to ruby-colored colloidal-Au suspension^[8] at room temperature, color changes were observed within several minutes.^[9] The spectral changes are shown in Figure 1c. It is clearly seen that the absorbance is highly dependent on the quantity of KI added. The native-surface plasmon band at 520 nm weakens and an absorption band in the red/infrared region (λ_{max} ca. 760 nm) appears and becomes more intense with increasing addition of KI solution. The weakening of the plasmon band is attributed to damping effects,^[6] whereas the new band indicates aggregation^[10a] and/or changes in the shape^[10b] of gold NPs.

TEM^[11] results correlate with the KI addition-dependent spectroscopic observations as shown in Figure 2. The native gold NPs are monodispersed, nearly spherical in shape, with an average diameter of 12 nm, and well separated (see Supporting Information). When a small amount of KI was added, the TEM image shows the presence of NP aggregates, each consisting of hundreds of individual NPs that are in close contact (Figure 2a–c). These individual NPs of aggregates are predominantly spherical with a diameter of 20–30 nm. However, in some domains we found some gold NPs smaller than the original spherical gold NPs (Figure 2c). We attribute these changes in the dimensions of the gold NPs to energetic injection, and the energy source is electron injection by the reductive chemisorption of iodide ions^[3] ($\text{I}^- - \text{e}^- \rightarrow \text{I}_{(\text{adsorbed})} + \text{e}^-$). Similar energetic-injection-induced fusion,^[12] fragmentation,^[13] and dissolution^[14] of NPs has been described. Upon

[*] Prof. S. Dong, Prof. E. Wang, W. Cheng
State Key Laboratory of Electroanalytical Chemistry Changchun
Institute of Applied Chemistry
Chinese Academy of Sciences, Changchun, Jilin 130022 (P.R. China)
Fax: (+86) 431-5689711
E-mail: dongsj@ciac.jl.cn
ekwang@ns.ciac.jl.cn

[**] This work was supported by the National Natural Science Foundation of China. (No. 29835120, No. 29975028).

Supporting information for this article is available on the WWW under <http://www.angewandte.org> or from the author.

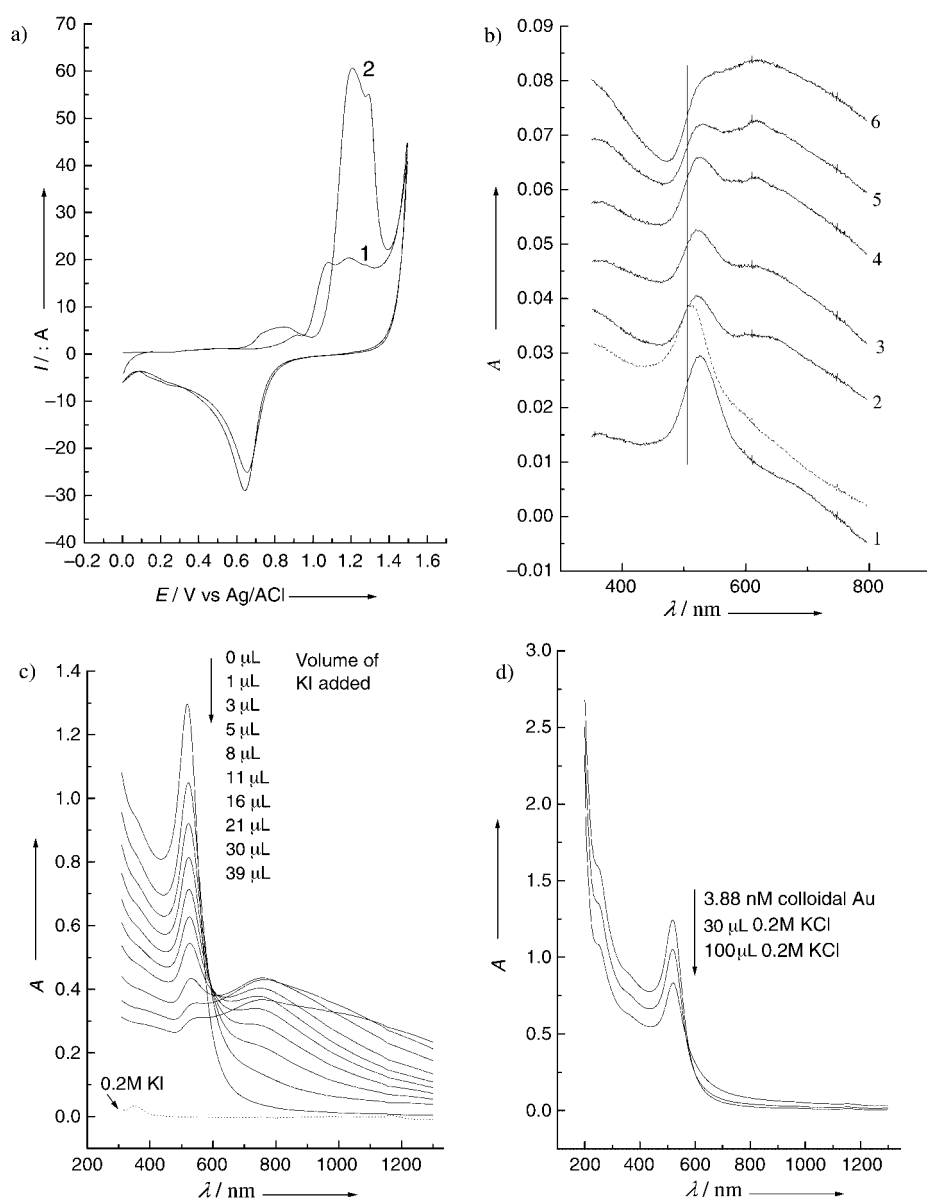


Figure 1. a) Cyclic voltammograms in 0.5 M H_2SO_4 of NP submonolayers on APTMS-modified ITO before (1) and after (2) iodine adsorption. Scan rate is 50 mVs^{-1} . b) Absorbance spectra monitoring of the construction of iodine-bound ITO-surface-bound-NP nanostructured assemblies. The stepwise derivatizing cycles with Au colloid and 1 mM KI are labeled beside curves. The dotted line shows the absorbance of NP submonolayers on APTMS-modified ITO. c) UV/Vis absorption changes of colloidal Au (1 mL, 3.88 nm) upon addition of different amounts of aqueous 0.2 M KI solutions. d) UV/Vis absorption changes of colloidal Au (1 mL, 3.88 nm) upon addition of different amounts of aqueous 0.2 M KCl solutions.

increasing the KI addition, the aggregation becomes more extensive (Figure 2d,e). Excess KI addition ($\geq 50 \mu\text{L}$) leads to a decrease of both absorption bands, and the whole broad absorption band is extended into infrared region.^[15] Under these conditions, many nanocrystals with various geometries could be seen in the TEM (Figure 2f). Comparison of the optical response with the corresponding TEM morphology reveals that the appearance of the broad absorbance band is actually mirrored by the appearance of the anisometric nanocrystals.^[10b] Previous studies indicate that collective optical, electronic properties^[1–3] are dictated by aggregate

size,^[10a] particle shape,^[10b] inter-particle distance,^[10a,16] and damping effects.^[6] Here, optical spectra and TEM, support the idea that coupling aggregation and damping effects dictate optical responses in low KI concentration and anisometric nanocrystal shape determines the optical responses in high KI concentration.

It is clearly noted from TEM that iodine-induced gold-NP aggregation is different from that described in reference [1]. It resembles photoinduced conversion^[17] of silver nanospheres into nanoprisms, where an energetic injection process was also involved. In our system, the energy source is the electron injection which results from iodide reduction. Such electron-transfer processes are not unusual, and it has been indicated in C_{60} -mediated aggregation.^[18] Based on these experimental results and the previous studies,^[17,18] an iodine chemisorption-induced aggregating/fusing mechanism is given in Figure 3. The chemisorbed iodine atoms on NPs would neutralize NP surface charge, and as a result, increase the van der Waals attractive forces among these iodine-coated NPs which would lead to aggregate generation. The iodine atoms might be still associated with these NP aggregates to keep structural stability. The fusion/fragmentation is at the expense of the original gold NPs, this situation is supported by the presence of an isosbestic point in Figure 1c. Excess KI addition results in nearly complete fusion of the gold NPs. The fusing process is similar to Ostwald ripening (i.e. particle growth through the exchange of “monomer” between particles), and KI addition enhances the rate of the Ostwald ripening process. Thus, small amounts of a water-soluble gold-iodide/iodine might exist.

Strong interaction of iodides and gold NPs is reminiscent of the strategy of Willner and co-workers^[3a,10a] for the fabrication of surface-bound nanostructured assemblies on solid supports. Interestingly, repeated treatment of APTMS-modified ITO with citrate-stabilized colloidal Au and 1 mM KI results in similar nanostructure generation, which is shown by spectral observations (Figure 1b). The above discussion demonstrates that the immersion of primary gold NPs

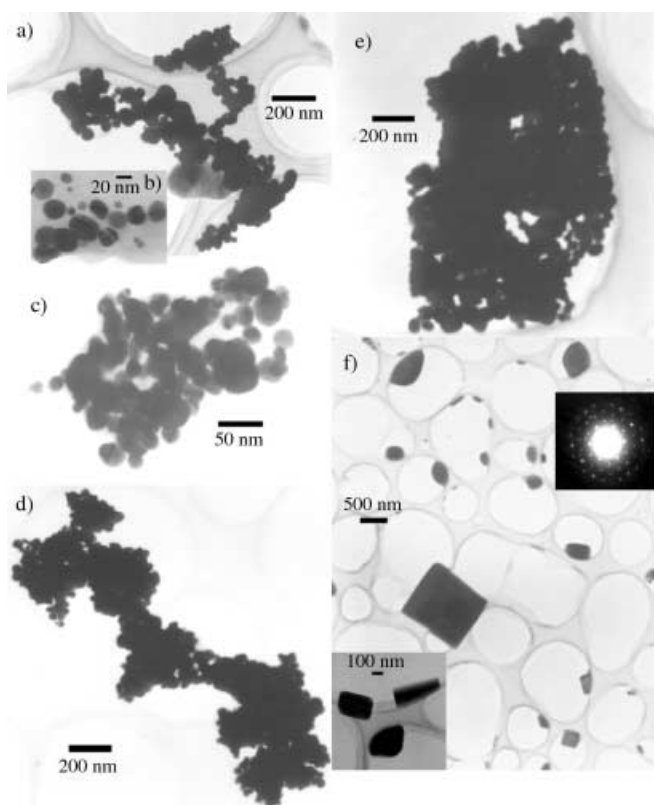


Figure 2. Representative morphological changes of TEM micrographs for colloid Au (1 mL, 3.88 nm) upon addition of different amounts of 0.2 M KI solutions: 6 μ L (a–c), 18 μ L (d–e), 60 μ L (f). Inset of (f) top: electron diffraction pattern analysis. The spot array, diagnostic of a hexagonal structure, is from the [111] orientation of the largest cubic platelet lying flat on the substrate with the top facet perpendicular to the electron beam, bottom: enlargement.

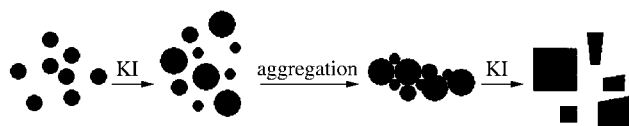


Figure 3. Schematic aggregating/fusing mechanism of gold NPs upon KI addition.

submonolayers into dilute KI leads to iodine-atom-monolayer formation on these immobilized NPs (Figure 1b, curve 1). This adsorbed iodine lowers the surface charge of the immobilized NPs significantly, as a result, additional gold NPs can be “glued” together upon immersing them in Au colloid. Formation of a second NP layer is demonstrated by the decrease of the plasmon absorbance and the appearance of second coupled plasmon absorbance band arising from the close contact of NPs (curve 2).^[3,10a] As the treating times are increased, the coupled-band strengthens (curves 3–6), which indicates that the coupling interactions become longer-range.^[3,10a] Previously, fabrication of surface-bound nanostructures was based on electrostatic or covalent interactions, whereas van der Waals attractive forces could be the driving forces for the surface-bound nanostructure formation in this study.

In conclusion, this study demonstrates for the first time that iodine chemisorption takes place on gold NPs. Compared with previous aggregating studies,^[1,2] both aggregation and fusion/fragmentation of NPs were observed by TEM upon KI addition. We propose that the physical origin of the fusion/fragmentation of gold NPs is energetic injection, which fits with these previous studies.^[12–14,17] The driving force of aggregation should be van der Waals attractive force. It is found that I-linked surface-bound-NP nanostructure can be fabricated by a layer-by-layer deposition techniques. This observation shows that crosslinkers are not confined to oligocations.^[3,10a] It is expected that this study might be instructive for testing the relationship between collective optical responses of metal NPs^[1–3] and individual NPs, and could find application in nanoscale electronics and photonics.

Experimental Section

Reagents: analytical grade $[\text{HAuCl}_4] \cdot 3\text{H}_2\text{O}$, trisodium citrate, KI, and KCl were all purchased from commercial vendors (Aldrich) and used as received. Solutions were prepared from ultrapure water purified with Milli-Q plus system (Millipore Co.), its resistivity was over 18 M Ω cm.

Instrumentation: all electrochemical experiments were carried out on Autolab PGSTAT30 potentiostat (Utrecht, Netherlands) in a conventional one-compartment cell. The cell was housed in a homemade Faraday cage to reduce stray electrical noise. The electrochemical measurements were performed using standard three-electrode systems. A Ag/AgCl electrode was used as the reference electrode, a Pt foil as the counter electrode, and the O-rings with 6 mm inner diameter were used to seal the ITO slides for all electrochemical experiments (geometry area is ca. 0.283 cm²). Optical spectra were acquired using Cary 500 UV-visible NTR spectrometer (Varian, USA). TEM samples were examined by using JEOL 2010 transmission electron microscopy operated at 200 kV.

Synthesis of 3.88 nm colloidal Au: Typically, aqueous solutions of $[\text{HAuCl}_4]$ (≈ 0.5 mL 1%) were diluted (to 70 mL), then the mixed solutions were heated to nearly boiling. Afterwards, aqueous trisodium citrate solutions (≈ 1.3 mL) were injected into the stirring system. The color changes were noted within several minutes, and a ruby-colored solution was obtained finally. The concentration of gold NPs was calculated to be ≈ 3.88 nm by assuming an average 12 nm diameter for all NPs.

Received: May 17, 2002

Revised: August 23, 2002 [Z19327]

- [1] a) A. K. Boal, F. Ilhan, J. E. DeRouchey, T. Thurn-Albrecht, T. P. Russell, V. M. Rotello, *Nature* **2000**, 404, 746–748; b) R. P. Andres, J. D. Bielefeld, J. I. Henderson, D. B. Janes, V. R. Kolagunta, C. R. Kubiak, W. J. Mahoney, R. G. Osifchin, *Science* **1996**, 273, 1690–1693; c) C. A. Mirkin, R. L. Letsinger, R. C. Mucic, J. J. Storhoff, *Nature* **1996**, 382, 607–609; d) A. P. Alivisatos, K. P. Johnsson, X. G. Peng, T. E. Wilson, C. J. Loweth, Jr., M. P. Bruchez, P. G. Schultz, *Nature* **1996**, 382, 609–611; e) M. Brust, D. Bethell, D. J. Schiffrin, C. J. Kiely, *Adv. Mater.* **1995**, 7, 795–797; f) S. Mann, W. Shenton, M. Li, S. Connolly, D. Fitzmaurice, *Adv. Mater.* **2000**, 12, 147–150; g) Y. Jin, S. Dong, *Angew. Chem.* **2002**, 114, 1082–1086; *Angew. Chem. Int. Ed.* **2002**, 41, 1040–1044.
- [2] J. P. Novak, D. L. Feldheim, *J. Am. Chem. Soc.* **2000**, 122, 3979–3980.

- [3] a) A. N. Shipway, E. Katz, I. Willner, *ChemPhysChem* **2000**, *1*, 18–52; b) W. Cheng, J. Jiang, S. Dong, E. Wang, *Chem. Commun.* **2002**, 16, 1706.
- [4] H. O. Finklea in *Electroanalytical Chemistry*, Vol. 19 (Eds.: A. J. Bard), Marcel Dekker, New York, **1996**, pp. 185–187.
- [5] R. G. Freeman, K. C. Grabar, K. J. Allison, R. M. Bright, J. A. Davis, A. P. Guthrie, M. B. Hommer, M. A. Jackson, P. C. Smith, D. G. Walter, M. J. Natan, *Science* **1995**, *267*, 1629–1632.
- [6] P. Mulvaney, *Langmuir* **1996**, *12*, 788–800.
- [7] a) S. I. Cumberland, G. F. Strouse, *Langmuir* **2002**, *18*, 269–276; b) F. W. Vance, B. I. Lemon, J. T. Hupp, *J. Phys. Chem. B* **1998**, *102*, 10091–10093.
- [8] Gold colloids were prepared by the conventional citrate reduction of $[\text{HAuCl}_4]$ in water at near-boiling temperature. See G. Frens, *Nature* **1973**, *241*, 20.
- [9] The colloid became light-blue upon addition of a small amount of KI and light-gray upon addition of excess KI.
- [10] a) A. N. Shipway, M. Lahav, R. Gabai, I. Willner, *Langmuir* **2000**, *16*, 8789–8795; b) J. Wiesner, A. Wokaun, *Chem. Phys. Lett.* **1989**, *157*, 569–575.
- [11] TEM examination was conducted by applying a drop of the samples to carbon-coated copper grids in contact with filter paper. The solvent was quickly wicked away by the filter paper, preventing particle agglomeration.
- [12] Y. Takeuchi, T. Ida, K. Kimura, *J. Phys. Chem. B* **1997**, *101*, 1322–1327.
- [13] a) H. Kurita, A. Takami, S. Koda, *Appl. Phys. Lett.* **1998**, *72*, 789; b) A. Takami, H. Yamada, K. Nakano, S. Koda, *Jpn. J. Appl. Phys.* **1996**, *35*, L781.
- [14] Y. Nakao, *J. Chem. Soc. Chem. Commun.* **1994**, 2067.
- [15] Precipitation is not found, even after several days later.
- [16] a) B. Kim, S. L. Tripp, A. Wei, *J. Am. Chem. Soc.* **2001**, *123*, 7955–7956; b) J. J. Storhoff, A. A. Lazarides, R. C. Mucic, C. A. Mirkin, R. L. Letsinger, G. C. Schatz, *J. Am. Chem. Soc.* **2000**, *122*, 4640–4650.
- [17] R. C. Jin, Y. W. Cao, C. A. Mirkin, K. L. Kelly, G. C. Schatz, J. G. Zheng, *Science* **2001**, *294*, 1901–1903.
- [18] M. Brust, C. J. Kiely, D. Bethell, D. J. Schiffrin, *J. Am. Chem. Soc.* **1998**, *120*, 12367–12368.

Ruthenium Metallo dendrimers

Dendritic Stars by Ring-Opening-Metathesis Polymerization from Ruthenium–Carbene Initiators

Sylvain Gatard, Sylvain Nlate, Eric Cloutet, Georges Bravic, Jean-Claude Blais, and Didier Astruc*

Dendrimers are a rich and appealing field of polymer chemistry.^[1] Organic polymerization from dendritic initiators also offers a route to highly branched polymers, and indeed these have been obtained, amongst other methods, by atom transfer radical polymerization (ATRP), anionic polymerization at a focal point of dendrons,^[2] and cationic polymerization of styrene using star-shaped initiators.^[3] Our goal was to synthesize dendritic stars by polymerization at the branch termini of a core. Therefore, we investigated the synthesis of new stable ruthenium–carbene^[4–8] dendrimers^[9,10] that would be able to catalyze subsequently the ring-opening-metathesis polymerization (ROMP) of norbornene.^[11] Only a few metal–carbene dendrimers are known: these are tetra-branched ruthenium catalysts recently reported by the groups of Hoveyda,^[4] van Koten,^[5] and Verdonck.^[6]

Herein, we report: a) the synthesis of new ruthenium–carbene complexes containing a chelating diphosphane, b) by modeling a dendritic branch, the reversible dimerization of these complexes in concentrated solutions, c) the extension of this synthetic route to three generations of dendritic ruthenium–carbene complexes, d) the ROMP reactions of the latter with norbornene to form metallodendritic stars, and e) the remarkable dendritic effects on the dimerization and polymerization reactions.

We designed a system that should be stable enough to support the dendritic structure and yet be reactive enough for ROMP. Therefore, we selected a chelating diphosphane–ruthenium–carbene framework. The strategy is based on recent breakthroughs. Hoveyda^[4] modified the Grubbs catalyst $[\text{RuCl}_2(\text{PCy}_3)_2](\text{CHPh})$ ^[7,10] (Cy = cyclohexyl) by introducing an isopropoxy substituent at the *ortho* position of the benzyldiene ligand such that the hemilabile chelating ether ligand replaces one phosphane. We chose the PPh_3 version of this system as the PPh_3 group can be substituted by a chelating diphosphane unit containing a dendritic branch. Hofmann

[*] Prof. Dr. D. Astruc, Dr. S. Gatard, Dr. S. Nlate
LCOO, UMR CNRS 5802
Université Bordeaux I
33405 Talence Cedex (France)
Fax: (+33) 5-5684-6646
E-mail: d.astruc@lcoo.u-bordeaux.fr
Dr. E. Cloutet
LCPO, ENSCPB
Université Bordeaux I, 33607 Pessac Cedex (France)
Dr. G. Bravic
ICMCB, 33608 Pessac Cedex (France)
Dr. J.-C. Blais
LCSOB, UMR CNRS 7613
Université Paris VI, 75252 Paris (France)